

深度调峰工况下大型汽轮发电机定子端部结构优化仿真研究

李敏洁¹, 刘轩东^{1*}, 白雪扬¹, 商高屹¹, 梅子杰¹, 李志军², 马党国²

(1. 西安交通大学 电工材料电气绝缘全国重点实验室, 陕西 西安 710049;

2. 华电电力科学研究院有限公司, 浙江 杭州 310030)

Simulation Study on Optimization of Stator End Structure for Large Steam Turbine Generators under Deep Peak Shaving Conditions

LI Minjie¹, LIU Xuandong^{1*}, BAI Xueyang¹, SHANG Gaoyi¹, MEI Zijie¹,
LI Zhijun², MA Dangguo²

(1. State Key Laboratory of Electrical Insulation and Power Equipment, Xi'an Jiaotong University,
Xi'an 710049, China;

2. Huadian Electric Power Research Institute Co., Ltd., Hangzhou 310030, China)

Abstract: [Objective] Under the dual-carbon target, coal-fired units are transitioning from operating under long-term stable loads to flexible operation. The deep peak shaving capability has become a critical indicator of the flexibility of coal-fired power units. However, deep peak shaving operations lead to rapid changes in the generator's hotspot temperatures, causing faults such as winding deformation, insulation wear, delamination, and wedge loosening. This paper investigates the operating state of the stator end of generators under deep peak shaving conditions. [Methods] Using COMSOL Multiphysics finite element analysis software, a multi-physics field coupling model for the stator winding was established, integrating electrical, magnetic, and mechanical fields. The vibration displacement of conductor bars and wedges was analyzed under two deep peak shaving conditions: rapid load variation and ultra-low load. Furthermore, to accelerate the adaptability of generators to deep peak shaving operation, two stator end structure optimization schemes were proposed. [Results] Simulation results showed that when the load changed at a rate of 5%/min, the vibration amplitudes of the straight section conductor bars, wedges, and slot exit conductor bars decreased by 21.19%, 99.7%, and 59.05%, respectively, compared to the original structure under rated

conditions. When the generator operated at 30% load, the displacement reductions were 72.46%, 99.997%, and 53.85%, respectively. [Conclusion] After structural optimization, the displacement amplitudes of the straight section conductor bars, wedges and slot exit conductor bars under extreme rapid load variation conditions are significantly reduced, confirming the effectiveness of the optimized structure.

Key words: deep peak shaving; stator end winding; conductor bar vibration; optimization of generator structure

摘要:【目的】双碳目标下,燃煤机组正由长期带稳定负荷运行转为灵活性运行,深度调峰能力是衡量燃煤机组灵活性运行的一项重要指标。但深度调峰运行会使得发电机热点温度快速变化,导致绕组变形、绝缘磨损、脱壳及槽楔松动等故障。本文针对深度调峰工况下发电机定子端部运行状态展开研究。【方法】基于 COMSOL Multiphysics 有限元分析软件,建立了电-磁-力多物理场耦合的定子绕组本体模型,分析了快速变负荷与超低负荷两种深度调峰工况下的线棒与槽楔振动位移情况。进一步地,为了加快发电机适应深度调峰运行,提出了两种定子端部结构优化方案。【结果】仿真结果表明,当负荷以 5%/min 速率变化时,直线段线棒、槽楔和出槽口线棒位移相比于优化前额定工况下的振动幅度分别降低了 21.19%、99.7% 和 59.05%。当发电机处于 30% 运行工况下,其位移分别降低了 72.46%、99.997% 和 53.85%。【结论】发电机结构优化后处于极端快速变负荷工况下,直线段线棒、槽楔和出槽口线棒位移幅度显著降低,验证了优

基金项目:中国华电集团有限公司“揭榜挂帅”项目
(CHDKJ22-01-108)

Project “Unveiling and Commanding” of China Huadian Corporation Limited (CHDKJ22-01-108)

化结构的有效性。

关键词: 深度调峰; 定子端部绕组; 线棒振动; 发电机结构优化

0 引言

“碳达峰, 碳中和”战略目标下, 我国正加快构建“清洁低碳, 安全高效”的能源体系, 可再生能源占比逐步提高^[1]。但是, 风能、太阳能等可再生能源大多具有间歇性与波动性, 大规模并网给电力系统带来巨大冲击, 造成燃煤等发电机组需配合新能源并网而不断改变自身状态, 频繁调峰、调频、变负荷及降低负荷运行等^[2]。这也就意味着燃煤发电机组的运行特征将由稳态运行转向灵活调峰运行。大型汽轮发电机运行期间, 定子端部绕组会受到电磁力作用发生振动, 此振动通常在材料可承受范围内。而深度调峰运行工况会使得绕组振动位移频繁变化。汽轮发电机因不适应机组深度调峰运行, 出现了线棒与定子槽楔松动引起的绝缘与铁心磨损等一系列问题^[3-6]。相关研究表明, 当发电机处于频繁变负荷、超低负荷等深度调峰工况运行时, 定子线棒槽楔松动程度增加、振动加剧以及绝缘材料发生脱壳等故障^[7-10]。但是, 以上研究皆是从理论角度推断出深度调峰工况可能对定子结构造成的影响, 并无电磁力、振动位移变化等数据的支撑。

大型汽轮发电机定子端部电磁力及振动的求解方法一般分为解析法和数值法。早期对端部漏磁场的研究主要应用解析法^[11-14]。近年来用数值分析方法进行电磁场计算的理论得到了较快的发展^[15-18]。胡宇达基于电磁场基本方程, 计算了定子端部在瞬态和稳态情况下的磁通密度和端部绕组的受力分布^[19]。Khan 给出了定子端部绕组磁场分布的表达式, 分析了定子端部绕组的电磁振动^[11]。Scott 在受力分析的基础上分析了功率因数对力的影响, 并分析了负荷对端部电磁力的影响^[20]。姚肖方建立了定子端部绕组电磁力计算数学模型, 运用 Matlab 软件计算了不同位置处的电磁力密度^[21]。上述学者详细分析了定子端部磁场分布情况, 并得到绕组电磁力密度结果。但是以上研究仅针对发电机额定运行工况或三相短路等故障工况下定子端部磁场分布, 并未考虑

深度调峰对发电机定子端部磁场分布造成的影响。当前对于深调工况下发电机定子端部绕组运行状态研究较少, 因此, 本文结合发电机定子端部实际结构, 研究深度调峰运行工况下, 定子端部绕组所受电磁力与振动位移变化。

为提高大型汽轮发电机在深度调峰工况下的安全稳定运行能力, 本文建立了汽轮发电机定子绕组电-磁-力多物理场耦合模型, 分析了深度调峰工况下定子端部绕组与槽楔在电磁力作用下的振动位移变化。进一步地, 对定子端部提出直线段与出槽口结构优化方案。对比优化前后的定子端部线棒、槽楔位移幅度来验证优化方案的有效性。

1 定子端部绕组电-磁-力多场耦合模型构建

1.1 数学模型

汽轮发电机正常运行时, 其定转子之间气隙大小变化会引起气隙磁导的变化, 单位面积的气隙磁导与磁势相乘可得到气隙磁密。气隙大小与气隙磁势的关系如图 1 所示。

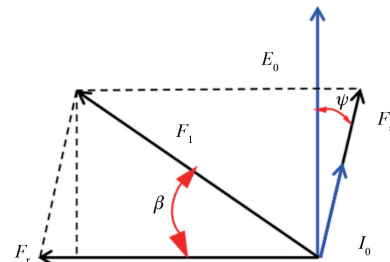


图 1 发电机额定工况下气隙磁势

Fig. 1 Air-gap magnetomotive force under rated conditions of the generator

额定运行工况下发电机气隙磁势可由电枢反应磁势与转子磁势计算得出, 如式(1)所示^[22]:

$$\begin{aligned} f(\alpha_m, t) &= F_r \cos(\omega_r t - \alpha_m) + \\ F_s \cos\left(\omega_r t - \alpha_m - \psi - \frac{\pi}{2}\right) &= \\ F_1 \cos(\omega_r t - \alpha_m - \beta) \end{aligned} \quad (1)$$

$$\begin{cases} F_1 = \sqrt{F_s^2 \cos^2 \psi + (F_r - F_s \sin \psi)^2} \\ \beta = \arctg \frac{F_s \cos \psi}{F_r - F_s \sin \psi} \end{cases} \quad (2)$$

式中: F_r 为转子磁势; F_s 为电枢反应磁势; F_1 为

合成磁势; $\omega = 2\pi f$ 为角速度; α_m 为机械角; ψ 为发电机内功角。

其单位面积气隙磁导控制方程为^[23]

$$\Lambda = \frac{\mu_0}{g} = \Lambda_0 \quad (3)$$

式中: μ_0 为真空磁导率; g 为发电机气隙径向长度。

式(1)与式(3)相乘得发电机额定运行工况下气隙磁密^[23]:

$$B(\alpha_m, t) = f(\alpha_m, t) \Lambda_0 = F_1 \cos(\omega_r t - \alpha_m - \beta) \Lambda_0 \quad (4)$$

为便于分析绕组受力,现对绕组进行编号,如图2所示。从A₁相的右侧开始,逆时针旋转,外侧线棒为S,内侧线棒为X。A₁相绕组编号为S₁~S₇,X₂~X₈。以此类推,获得所有绕组编号。

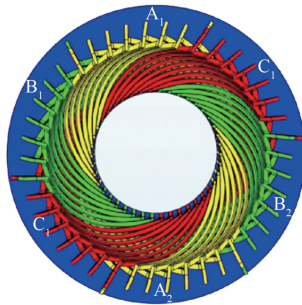


图2 定子绕组编号示意

Fig. 2 Numbering of stator windings

定子端部绕组由上下两层线棒构成,故汽轮发电机在额定运行工况下的定子端部绕组三相对称电流为

$$\begin{cases} I_A = i_a/2 = 0.5 \cdot I_m \sin(\omega t) \\ I_B = i_b/2 = 0.5 \cdot I_m \sin\left(\omega t - \frac{2\pi}{3}\right) \\ I_C = i_c/2 = 0.5 \cdot I_m \sin\left(\omega t + \frac{2\pi}{3}\right) \end{cases} \quad (5)$$

式中: $I_m = \sqrt{2}I$,其中 $I=17\,495.5\text{ A}$ 。

深度调峰运行主要表现在三个方面:一是机组快速变负荷;二是实现超低负荷运行;三是机组大幅度变负荷^[3]。本文采用电流激励模拟快速变负荷与超低负荷两种深调工况。

对于快速变负荷运行工况,当发电机负荷以 $a\%/\text{min}$ 速率下降时:

$$\begin{cases} I_A = 0.5 \cdot \left(I_m - \frac{a^{-2}}{60} \cdot t\right) \sin(\omega t) \\ I_B = 0.5 \cdot \left(I_m - \frac{a^{-2}}{60} \cdot t\right) \sin\left(\omega t - \frac{2\pi}{3}\right) \\ I_C = 0.5 \cdot \left(I_m - \frac{a^{-2}}{60} \cdot t\right) \sin\left(\omega t + \frac{2\pi}{3}\right) \end{cases} \quad (6)$$

对于超低负荷运行工况,当发电机以 $b\%$ 负荷运行时:

$$\begin{cases} I_A = 0.5 \cdot (I_m \cdot b^{-2}) \sin(\omega t) \\ I_B = 0.5 \cdot (I_m \cdot b^{-2}) \sin\left(\omega t - \frac{2\pi}{3}\right) \\ I_C = 0.5 \cdot (I_m \cdot b^{-2}) \sin\left(\omega t + \frac{2\pi}{3}\right) \end{cases} \quad (7)$$

定子端部绕组所受电磁力为

$$F = \int_v JB_\alpha dv \quad (8)$$

式中: v 为体积单元; J 为电流密度; B 为磁通密度。

假定定子绕组电流均匀分布,忽略绕组间的磁密影响,并将气隙磁密视为定子绕组的磁密,则其电磁力可表示为

$$F_i = B(\alpha_m, t) I_i L_w \quad (9)$$

式中: I 为绕组电流; L_w 为垂直于磁场方向的定子绕组长度; i 为第 i 个绕组线圈。

1.2 几何模型

发电机定子端部结构主要由绕组、槽楔、定子铁心和转子铁心组成,几何模型如图3所示。定子端部的参数如表1所示。在发电机运行过程中,直线段与出槽口处易发生振动磨损^[23-27],因此本文对以上两部分开展振动位移研究。其中,直线段主要由上下两层线棒、垫条和槽楔组成,出槽口由线棒绑扎带组成,如图4所示。

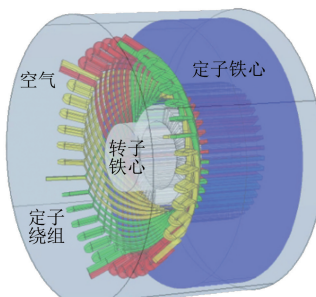


图3 定子端部几何模型

Fig. 3 Geometric model of stator end

表 1 定子端部基本参数

Tab. 1 Basic parameters of stator end

参数名称	参数值
额定功率/MW	600
额定电流/A	17 495.5
功率因数	0.9
频率/Hz	50
极对数	2
转速/(r·min ⁻¹)	3 000
定子槽数	42
每槽线棒数	2
定子绕组节距	17
转子槽数	32

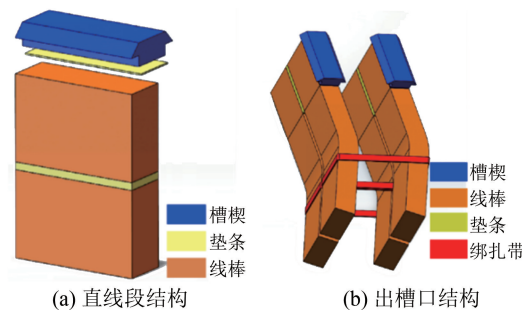


图 4 定子端部直线段与出槽口结构

Fig. 4 Structure of stator end straight and slot exit

1.3 边界条件

在电磁场中,通过对定子绕组施加电流激励,计算定子端部磁场分布,并得出线棒所受电磁力。在固体力学场中,将电磁力结果作为载荷映射至线棒上,并结合定子端部实际安装情况,设置槽楔与绑扎带固定边界。最终边界条件如表 2 所示。

表 2 定子端部直线段与出槽口边界条件设置

Tab. 2 Boundary condition settings for stator end straight section and slot exit

组件	边界条件
电磁场	S ₁ ~S ₇ 、S ₂₂ ~S ₂₈ 、X ₂ ~X ₈ 、X ₂₃ ~X ₂₉ 、S ₈ ~S ₁₄ 、S ₂₉ ~S ₃₅ 、X ₉ ~X ₁₅ 、X ₃₀ ~X ₃₆ 、S ₁₅ ~S ₂₁ 、S ₃₆ ~S ₄₂ 、X ₁₆ ~X ₂₂ 、X ₃₇ ~X ₁
	S ₁ I, X ₈ output I, I=I _A
	S ₈ input I, X ₁₅ output I, I=I _B
	S ₁₅ input I, X ₂₂ output I, I=I _C
	转子铁心
	槽楔
固体力学场	上层线棒
	下层线棒
	绑扎带

2 不同工况下定子端部位移仿真结果

2.1 额定工况下定子端部位移仿真结果

电磁力映射至直线段与出槽口处后得到位移结果如图 5 所示。针对绕组直线段而言,上层线棒位移较大。因为上层线棒靠近定子铁心,磁密大,由式(9)可知,此时线棒所受电磁力较大,因此振动幅度大于下层线棒。由图 5(b)可知,出槽口处的线棒振动位移大于直线段,越靠近外侧,位移值越大。因为在出槽口处,靠近内侧的线棒仍可在槽楔的紧固作用下减小振动,但槽楔对线棒的固定随着距离的增加而逐渐减小,外侧线棒仅依靠绑扎带固定,紧固力最弱,振动幅度最大。

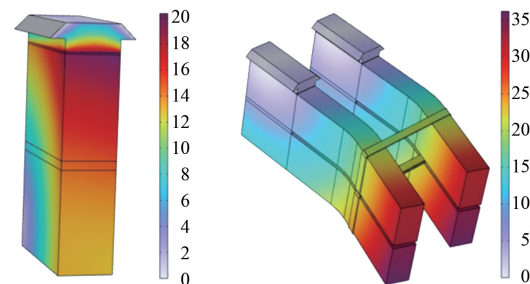


图 5 位移结果

Fig. 5 Displacement results

2.2 深调工况下定子端部位移仿真结果

由位移结果可知,直线段上层线棒、出槽口处外侧线棒位移值最大。因此,本文截取二者三维截线,表示线棒位移随调峰深度的变化趋势。为更好地分析槽楔在深度调峰工况下的变化规律,截取槽楔边线代表整体振动趋势。具体截线如图 6 所示。

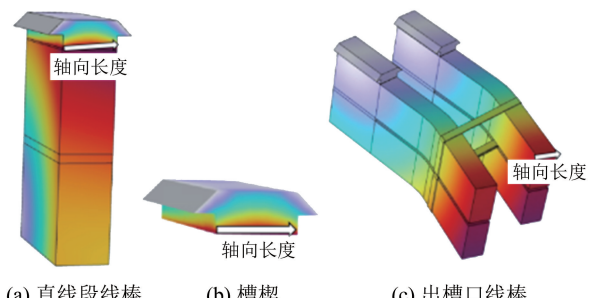


图 6 截线示意

Fig. 6 Cross-section illustration

根据中国电力设备管理协会标准,深度调峰工况的负荷变化率为 2%/min ~ 5%/min,负荷变

化范围为 30% ~ 100%^[28]。为更好地研究发电机的深度调峰范围,本文将负荷变化范围设置为 30% ~ 100%,并将负荷变化率扩展为 0.5%/min ~ 5%/min。

快速变负荷工况下线棒、槽楔位移情况如图 7 所示。直线段与出槽口处线棒振动位移分布均匀,而槽楔位移呈先增大后减小趋势,最大值出现在槽楔中部。因为在实际工程安装时,直线段线棒由垫条均匀压紧,出槽口线棒由绑扎带紧固,而

槽楔在楔入鸽尾槽时,仅由两侧斜面固定。三段处的位移均随着负荷变化速率的增加而增加。相较于额定运行工况,当负荷以 5%/min 速率变化时,直线段线棒位移最大值由 7.08 μm 上升至 201.39 μm,槽楔位移由 3.69 μm 上升至 104.97 μm,出槽口线棒位移由 14.80 μm 上升至 420.96 μm。最大变形量超过额定工况下变形量的 25 倍以上。

超低负荷工况下线棒、槽楔位移如图 8 所示。随着运行工况的下降,直线段线棒、槽楔与出槽口的位移均呈上升趋势。当发电机处于 30% 运行工况时,直线段线棒、槽楔、出槽口线棒最大位移

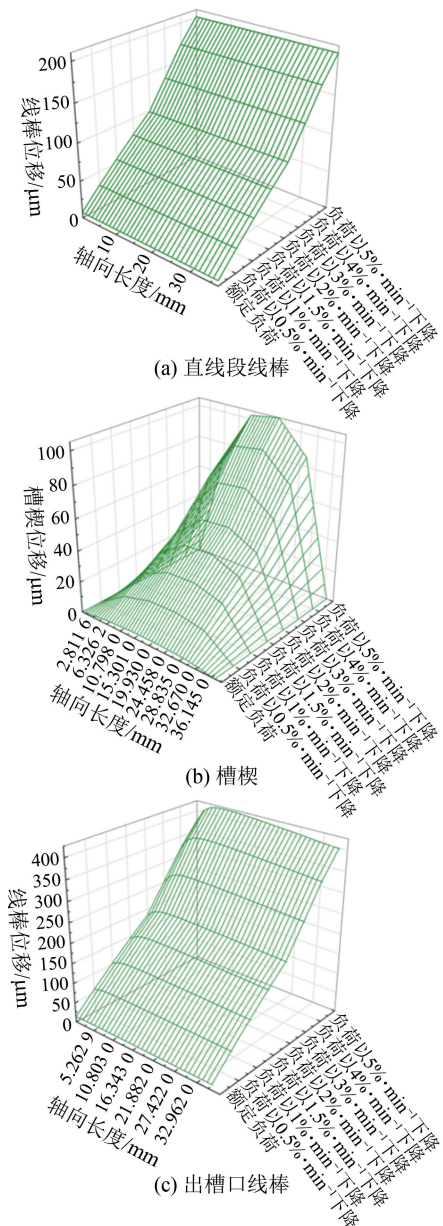


图 7 快速变负荷工况下位移结果

Fig. 7 Displacement results under rapid load variation conditions

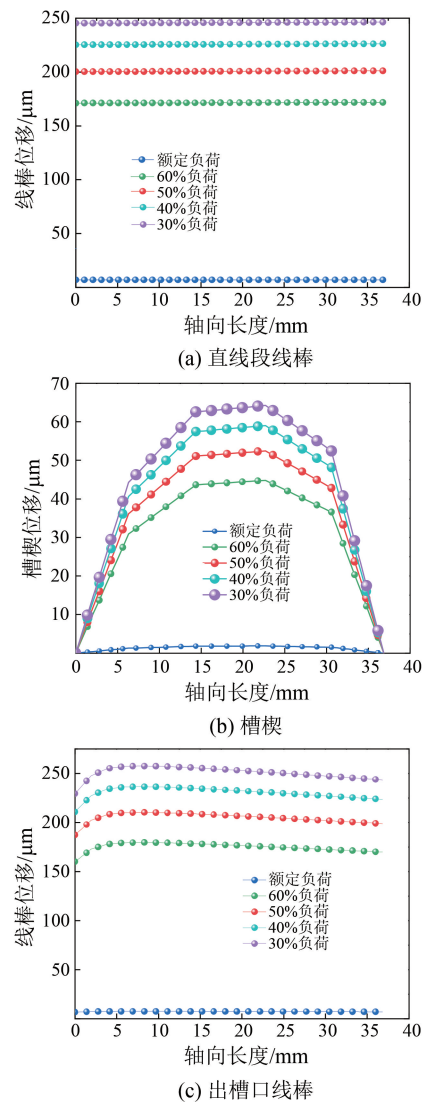


图 8 超低负荷工况下位移结果

Fig. 8 Displacement results under ultra-low load conditions

值高达 $246.43 \mu\text{m}$ 、 $64.22 \mu\text{m}$ 、 $257.55 \mu\text{m}$ 。相较于额定工况的位移值, 分别增加了 $239.35 \mu\text{m}$ 、 $60.53 \mu\text{m}$ 、 $242.75 \mu\text{m}$ 。

随着调峰程度的增加, 线棒振动幅值增大, 两类深度调峰工况下最大位移峰-峰值均超过国标^[29]要求位移峰-峰值(位移值×2) $250 \mu\text{m}$ 的 2 倍, 这将导致线棒与槽楔松动及绝缘材料磨损加剧等故障。因此, 必须对定子端部进行结构优化改造。

3 定子端部优化设计及仿真结果

3.1 定子端部结构优化设计

定子端部直线段结构优化如图 9 所示。在线棒与槽楔间填充波纹板, 并将“平槽楔+波纹板”的定子槽楔固定结构改为“斜槽楔+斜楔+波纹板”。一方面, 波纹板是一种新型的波纹状的玻璃纤维增强的槽内固定材料, 具有高弹性。将其放置在槽楔下, 以产生压向槽底的预紧力, 此时波纹板压缩伸展变形弹力压住线棒, 使其更加紧固, 在运行地电磁力振动下能保证电机定子线圈坚固牢靠。另一方面, “斜槽楔+斜楔+波纹板”的结构将使槽楔固定更紧固, 更适应于发电机调峰运行方式。

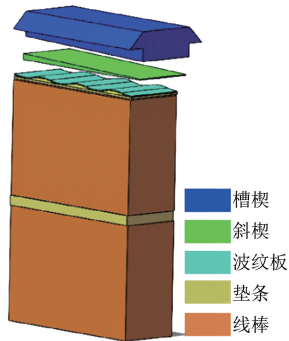


图 9 直线段结构优化

Fig. 9 Optimization of straight section structure

出槽口结构优化如图 10 所示。在出槽口相邻线棒间增设槽口块结构, 对定子线圈进行切向楔紧, 加强固定效果, 有效避免定子线圈槽口部位的松动磨损, 降低线圈绝缘磨损风险。

3.2 结构优化后定子端部绕组位移

结构优化后快速变负荷工况下线棒、槽楔位移情况如图 11 所示。位移仍随着负荷变化速率的增加而增加, 但程度大大减少。额定运行工况

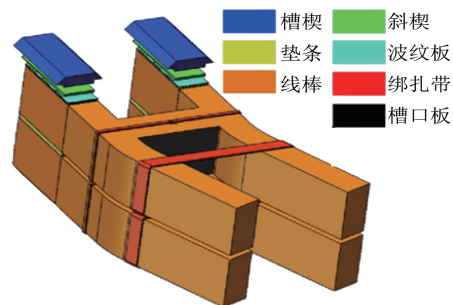
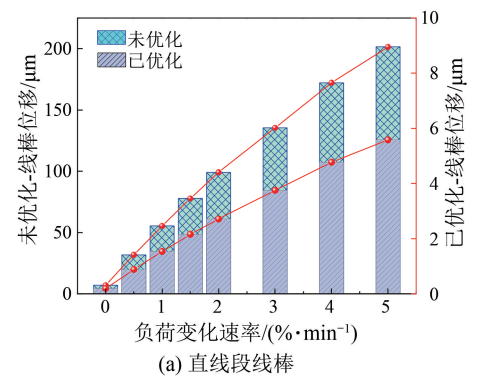
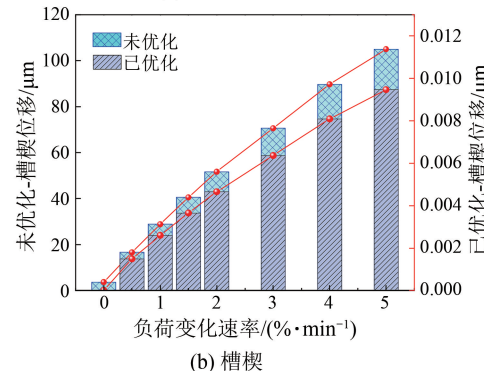


图 10 出槽口结构优化

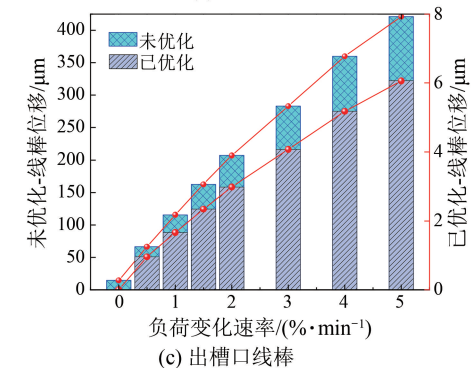
Fig. 10 Optimization of slot exit structure



(a) 直线段线棒



(b) 槽楔



(c) 出槽口线棒

图 11 快速变负荷工况下位移结果

Fig. 11 Displacement results under rapid load variation conditions

下, 直线段线棒、槽楔、出槽口线棒位移最大值为 $0.19 \mu\text{m}$ 、 $1.31 \times 10^{-5} \mu\text{m}$ 、 $0.008 \mu\text{m}$ 。即使负荷以

5%/min 速率变化,三段位移仅为 5.58 μm、0.0095 μm、6.06 μm,与结构优化前额定工况下的位移相比,分别降低了 21.19%、99.7%、59.05%。

结构优化后超低负荷工况下线棒、槽楔位移情况如图 12 所示。可以看出,位移大幅减小。即使发电机处于 30% 运行工况下,其直线段线棒位移、槽楔位移、出槽口线棒位移仅为 1.95 μm、 9.49×10^{-5} μm、6.83 μm。相比优化前额定工况下的位移值降低了 5.13 μm、3.6899 μm、7.97 μm,分别降低了 72.46%、99.997%、53.85%。

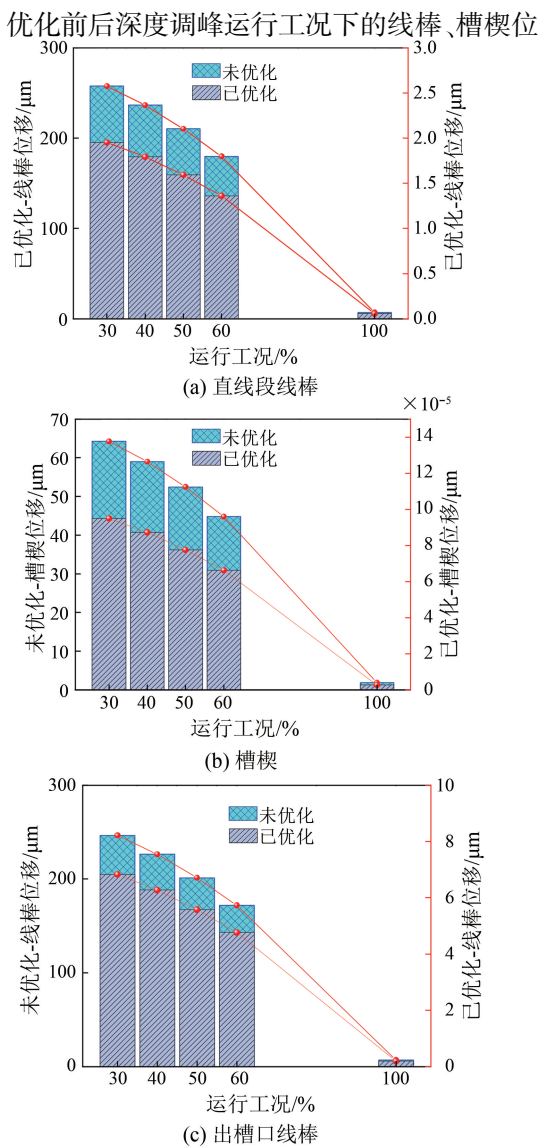


图 12 超低负荷工况下位移结果

Fig. 12 Displacement results under ultra-low load conditions

移峰-峰值如表 3 所示。随着调峰深度的增加,线棒和槽楔的振幅增大。当负荷变化率为 2%/min 时,出槽口线棒的位移峰-峰值为 414.24 μm。当发电机在 60% 负荷条件下运行时,其直线段线棒位移峰-峰值已达到 359.36 μm,超过或接近国标要求定子端部振动位移报警值(400 μm)^[29]。因此,结构优化前汽轮发电机能承受的负荷变化率范围为 0~2%/min,最低负荷为 60%。对定子端部结构进行优化改造后,即使负荷变化速率为 5%/min,三处位移峰-峰值仅为 11.16 μm、0.019 μm、12.12 μm。当负荷降低至 30% 运行工况,其位移峰-峰值仅为 3.90 μm、 1.89×10^{-4} μm、13.66 μm,远小于国家长期稳定运行位移峰-峰值标准(250 μm~400 μm)^[29]。故优化后的汽轮发电机可承受的变负荷速率范围为 0~5%/min,可承受 30%~100% 变化范围的运行负荷。

4 结语

燃煤机组灵活运行的方式已成为未来发展趋势,本文基于 COMSOL Multiphysics 有限元仿真软件建立了 600 MW 大型汽轮发电机定子端部电-磁-力耦合模型,应用矢量磁位法进行有限元计算得到定子端部线棒电磁力分布,并将电磁力映射至直线段与出槽口线棒处得到其振动位移结果。进一步提出发电机结构优化设计方案,加快发电机适应深度调峰运行,得出的主要结论:

(1) 随着调峰深度的增加,线棒与槽楔位移幅度增加,快速变负荷工况将导致位移幅值扩大 25 倍,最大位移值超过国标要求位移峰-峰值 250 μm 的 2 倍,严重威胁发电机安全稳定运行。

(2) 对定子端部进行结构优化改造可显著降低线棒与槽楔振动幅度,有效避免槽楔松动、线棒磨损等隐患故障的发生,使得发电机更好的适应深度调峰运行。优化后仿真结果表明,当负荷以 5%/min 速率变化时,其直线段线棒、槽楔和出槽口线棒位移相比于优化前额定工况下的振动幅度分别降低了 21.19%、99.7% 和 59.05%。当发电机处于 30% 运行工况下,其位移分别降低了 72.46%、99.997% 和 53.85%。

表 3 优化前后线棒、槽楔位移峰-峰值对比

Tab. 3 Comparison of peak-to-peak displacement of winding bar and slot wedge before and after optimization

运行工况	定子端部结构优化前			定子端部结构优化后		
	直线段线棒位 移峰-峰值/ μm	槽楔位移峰- 峰值/ μm	出槽口线棒位 移峰-峰值/ μm	直线段线棒位 移峰-峰值/ μm	槽楔位移峰- 峰值/ μm	出槽口线棒位 移峰-峰值/ μm
额定工况	14.16	7.38	29.60	0.38	2.62e-5	0.016
0.5%/min 负荷变化速率	63.76	33.23	133.27	1.77	0.003	1.92
1%/min 负荷变化速率	110.74	57.72	231.46	3.07	0.005	3.33
1.5%/min 负荷变化速率	155.59	81.10	325.24	4.31	0.007	4.68
2%/min 负荷变化速率	198.18	103.30	414.24	5.43	0.009	5.96
3%/min 负荷变化速率	270.82	141.16	566.08	7.51	0.013	8.15
4%/min 负荷变化速率	344.20	179.41	719.48	9.54	0.016	10.36
5%/min 负荷变化速率	402.78	209.94	841.92	11.16	0.019	12.12
60% 运行负荷	359.36	89.61	343.86	2.72	1.32e-4	9.53
50% 运行负荷	420.58	104.88	402.42	3.19	1.55e-4	11.16
40% 运行负荷	473.10	117.92	452.68	3.58	1.74e-4	12.55
30% 运行负荷	492.86	128.44	515.10	3.90	1.89e-4	13.66
可行域	负荷变化速率:0~2%/min 低负荷运行范围:60%~100%			负荷变化速率:0~5%/min 低负荷运行范围:30%~100%		

参 考 文 献

- [1] 国家能源局. 2023 年全国电力工业统计数据 [R]. 北京: 国家能源局, 2023.
- National Energy Administration. 2023 national electric power industry statistical data [R]. Beijing: National Energy Administration, 2023.
- [2] 国家发展改革委,国家能源局. 关于印发《“十四五”现代能源体系规划》的通知[R]. 北京: 国家发展改革委, 2022.
- National Development and Reform Commission, National Energy Administration. Notice on issuing the "14th Five Year Plan for Modern Energy System" [R]. Beijing: National Development and Reform Commission, 2022.
- [3] 赵永亮, 许朋江, 居文平, 等. 燃煤发电机组瞬态过程灵活高效协同运行的理论与技术研究综述 [J]. 中国电机工程学报, 2023, 43(6): 2080-2100.
- ZHAO Y L, XU P J, JU W P, et al. Overview of theoretical and technical research on flexible and efficient synergistic operation of coal-fired power units during transient processes [J]. Proceedings of the CSEE, 2023, 43(6): 2080-2100.
- [4] 彭凌云. 某大型汽轮发电机定子端部松动对策 [J]. 上海大中型电机, 2018, (1): 47-49.
- PENG L Y. Countermeasures for stator end looseness of a large turbo-generator [J]. Shanghai Medium and Large Electrical Machines, 2018, (1): 47-49.
- [5] 李光明. 600 MW 汽轮发电机端部绝缘松动原因分析及处理 [J]. 设备管理与维修, 2019, (7): 55.
- LI G M. Reason analysis and treatment of end insulation looseness of 600 MW turbo-generator [J]. Plant Maintenance Engineering, 2019, (7): 55.
- [6] 董朋, 袁超, 封建宝, 等. 一起 1 000 MW 汽轮发电机转子匝间短路故障诊断分析 [J]. 大电机技术, 2018, 48(3): 16-19.
- DONG P, YUAN C, FENG J B, et al. Diagnosis and analysis of interturn short circuit fault in rotor of a 1 000 MW turbine generator [J]. Large Electric Machine and Hydraulic Turbine, 2018, 48(3): 16-19.
- [7] 江建明. 煤电灵活性运行对汽轮发电机的影响 [J]. 电力科技与环保, 2023, 39(2): 95-103.
- JIANG J M. The influence of flexible operation of coal power on turbine generator [J]. Electric Power Technology and Environmental Protection, 2023, 39(2): 95-103.
- [8] 姜永辰. 深度调峰对 660 MW 水氢氢汽轮发电机的影响分析及灵活性改造 [J]. 机电信息, 2023, (17): 48-51.
- JIANG Y C. Analysis of the impact of deep peak shaving on a 660 MW hydrogen-hydrogen turbine generator and its flexibility modification [J]. Mechanical and Electrical Information, 2023, (17): 48-51.
- [9] 刘(王卜). 负荷增减速速度对汽轮机的影响 [J].

- 四川电力技术, 1983, (4): 6-8+5.
- LIU W B. Influence of load increase and decrease rate on turbo-generator [J]. Sichuan Electric Power Technology, 1983, (4): 6-8+5.
- [10] 杨国龙, 陈文学, 令红兵. 燃煤机组新运行方式对在役汽轮发电机的影响 [J]. 大电机技术, 2018, (5): 48-53.
- YANG G L, CHEN W X, LING H B. The influence of new operation mode of coal-fired uniton steam turbine generator in service [J]. Large Electric Machine and Hydraulic Turbine, 2018, (5): 48-53.
- [11] KHAN G K M, BUCKLEY G W, BROOKS N. Calculation of forces and stresses on generator end-windings-Part I: Forces [C]. IEEE Transactions on Energy Conversion, 1989, 4(4): 661-669.
- [12] 单继聪. 大型汽轮发电机定子端部绕组电磁力的解析计算 [D]. 杭州: 浙江大学, 2008.
- SHAN J C. Study on electromagnetic forces of end windings in large turbo-generators [D]. Hangzhou: Zhejiang University, 2008.
- [13] 刘浩, 任华芝. 作用在同步电机定子绕组线棒上的电动力计算 [J]. 大电机技术, 2000, 30(1): 27-29.
- LIU H, REN H Z. Electrodynamic force calculation acting on the rods of the stator windings of a synchronous motor [J]. Large Electric Machine and Hydraulic Turbine, 2000, 30(1): 27-29.
- [14] HU Y D, QIU J J, TA N. Nonlinear electromagnetic vibration of turbo-generator stator end winding [C] // 2004 the Eleventh World Congress in Mechanism and Machine Science, Qinhuangdao, 2004.
- [15] 姚若萍, 候小全, 饶芳权. 大型水轮发电机在各种工况下的端部磁场计算 [J]. 上海交通大学学报, 2002, 36(2): 234-236+242.
- YAO R P, HOU X Q, RAO F Q. New approach for field computation in the end zone of hydro-generators [J]. Journal of Shanghai Jiaotong University, 2002, 36(2): 234-236+242.
- [16] 梁艳萍, 陆永平, 朱宽宁, 等. 汽轮发电机失磁异步运行时转子端部漏磁参数与涡流损耗的分析计算 [J]. 中国电机工程学报, 2004, 24(11): 112-115.
- LIANG Y P, LU Y P, ZHU K N, et al. Calculation of leakage reactance and eddy current losses in the rotor end region of large turbogenerator at asynchronous operation [J]. Proceedings of the CSEE, 2004, 24(11): 112-115.
- [17] 张甲. 大型汽轮发电机端部绕组电动力三维有限元分析 [D]. 杭州: 浙江大学, 2008.
- ZHANG J. Three-dimensional finite element analysis of electromagnetic forces acting on the end winding of large turbo-generator [D]. Hangzhou: Zhejiang University, 2008.
- [18] 长野进. 大容量隐极同步电机定子端部绕组振动的研究——电磁力计算精度的提高和绝缘老化的评价 [J]. 国外大电机, 2009, (1): 36-42+48.
- CHANG Y J. Research on stator end winding vibration of large-capacity hidden electrode synchronous motor-improvement of the accuracy of electromagnetic force calculation and evaluation of insulation aging [J]. Foreign Large Electrical Machines, 2009, (1): 36-42+48.
- [19] 胡宇达, 邱家俊. 大型汽轮发电机定子端部绕组整体结构的电磁振动 [J]. 中国电机工程学报, 2003, 23(7): 93-98.
- HU Y D, QIU J J. Electromagnetic vibration of integrity end winding of large turbo-generator stator [J]. Proceedings of the CSEE, 2003, 23(7): 93-98.
- [20] SCOTT D J, SALON S J, KUSIK G L. Electromagnetic forces on the armature end windings of large turbine generators I-steady state conditions [J]. IEEE Transactions on Power Apparatus and Systems, 1981, PAS-100(11): 4597-4603.
- [21] 姚肖方. 汽轮发电机定子绕组端部受力特性分析 [D]. 北京: 华北电力大学, 2013.
- YAO X F. Characteristic analysis of the forces acted on stator end windings of turbo-generator [D]. Beijing: North China Electric Power University, 2013.
- [22] 孙悦欣. 发电机三维气隙偏心下定子及其绕组的力学特性分析 [D]. 北京: 华北电力大学, 2020.
- SUN Y X. Analysis on mechanical properties of stator and stator windings of generator under three dimensional air gap eccentricity [D]. Beijing: North China Electric Power University, 2020.
- [23] 齐瑞鹏. 汽轮发电机定子线棒磨损原因分析及处理方案 [J]. 上海大中型电机, 2023, (1): 48-50.
- QI R P. Cause analysis and treatment scheme of the wear of stator bar turbo-generator [J]. Shanghai Medium and Large Electrical Machines, 2023, (1): 48-50.

- [24] 侯建. 汽轮发电机定子端部松动的检修方法 [J]. 防爆电机, 2017, (5): 42-44.
- HOU J. Repair method of loosened stator end of turbine generator [J]. Explosion-Proof Electric Machine, 2017, (5): 42-44.
- [25] 王林刚, 王彦忠, 盛隆. 某 660 MW 大型汽轮发电机定子线棒股线断裂原因分析 [J]. 浙江电力, 2020, (2): 101-105.
- WANG L G, WANG Y Z, SHENG L. Cause analysis of strands breakage on generator stator bar of a 660 MW large steam turbine generator [J]. Zhejiang Electric Power. 2020, (2): 101-105.
- [26] 沈德华. 大型汽轮发电机线棒磨损原因分析与预防 [J]. 上海大中型电机, 2021, (4): 54-56.
- SHEN D H. Analysis on the reason and prevention of the wearing of the bar on large turbogenerator [J]. Shanghai Medium and Large Electrical Machines, 2021, (4): 54-56.
- [27] 邢超. 大型汽轮发电机定子绕组端部振动的研究 [D]. 保定: 华北电力大学, 2010.
- XING C. Research on the vibration turbo-generator stator end-windings [D]. Baoding: North China Electric Power University, 2010.
- [28] 中国电力设备管理协会标准. 煤电机组辅机及系统节能、供热和灵活性改造技术导则: T/CEEMA 001-2022 [S]. 北京: 中国电力设备管理协会, 2022.
- Standard of China Electric Power Equipment Management Association. Technical guide for energy conservation, heating, flexibility retrofits of coal-fired power steam turbines: T/CEEMA 001-2022 [S]. Beijing: China Electric Power Equipment Management Association, 2022.
- [29] 中国电器工业协会. 隐极同步发电机定子绕组端部动态特性和振动测量方法及评定: GB/T 20140-2016 [S]. 北京: 中华人民共和国国家质量监督检验检疫总局, 国家标准化管理委员会, 2016.
- China Electrical Equipment Industry Association. Measurement method and evaluation criteria of dynamic characteristic and vibration on stator end windings of cylindrical synchronous generators: GB/T 20140-2016 [S]. Beijing: General Administration of Quality Supervision, Inspection and Quarantine of the People's Republic of China, National Standardization Administration, 2016.

收稿日期: 2024-06-22

收到修改稿日期: 2024-10-08

作者简介:

李敏洁(2001-), 女, 硕士研究生, 研究方向为灵活调峰电机定转子多场耦合仿真技术, 2642528602@qq.com;

*通信作者: 刘轩东(1981-), 男, 博士, 教授, 研究方向为直流电力设备设计、气体绝缘与放电等离子体、高功率脉冲源及气体开关及应用, Liuxuand@mail.xjtu.edu.cn。

Simulation Study on Optimization of Stator End Structure for Large Steam Turbine Generators under Deep Peak Shaving Conditions

LI Minjie¹, LIU Xuandong^{1*}, BAI Xueyang¹, SHANG Gaoyi¹, MEI Zijie¹,
LI Zhijun², MA Dangguo²

(1. State Key Laboratory of Electrical Insulation and Power Equipment, Xi'an Jiaotong University,

Xi'an 710049, China;

2. Huadian Electric Power Research Institute Co., Ltd., Hangzhou 310030, China)

Key words: deep peak shaving; stator end winding; conductor bars vibration; optimization of generator structure

Under the strategic goal of “carbon peaking and carbon neutrality”, China is accelerating the construction of a “clean, low-carbon, safe and efficient” energy system, with the proportion of renewable energy gradually increasing. However, most renewable energy sources such as wind and solar are characterized by intermittency and volatility. Their large-scale grid integration has a significant impact on the power system, causing coal-fired and other power generation units to constantly adjust their operational states in response to renewable energy integration, frequent peak shaving, frequency regulation, load variation, and load reduction. This also means that the operational characteristics of coal-fired power generation units are shifting from steady-state operation to flexible peak shaving operation. During the operation of a large steam turbine generator, the stator end winding will vibrate under the action of electromagnetic forces, which is usually within the acceptable range of materials. Deep peak shaving operation conditions, however, will cause frequent changes in winding vibration displacement, as illustrated in Fig.1. Steam turbine generators have encountered a series of problems, including insulation and iron core wear, caused by loose winding bars and stator slot

wedges due to their inability to adapt to the deep peak shaving operation of the unit.



Fig. 1 Wear of stator slot wedge

Therefore, it is important to study the displacement changes of stator end winding vibration under deep peak shaving conditions to improve the safe and stable operational capability of large steam turbine generators under such conditions. This paper established a multi-physics field coupling model of the stator winding of a steam turbine generator. The displacement changes of the stator end winding and slot wedges under electromagnetic forces during deep peak shaving conditions were analyzed. Furthermore, an optimization scheme for the straight and slot exit section of the stator end was proposed. The displacement of the stator end bars before and after optimization was compared to verify the effectiveness of the optimization scheme.